Temperature and wavelength dependence of the Faraday ellipticity of lead-substituted gadolinium iron garnet films

P. Hansen, M. Rosenkranz, and K. Witter
Philips GmbH Forschungslaboratorium Hamburg, D-2000 Hamburg 54, Federal Republic of Germany
(Received 27 October 1981)

The Faraday ellipticity of epitaxial garnet films of composition $Y_3Fe_5O_{12}$ and $Gd_{3-x}Pb_xFe_{5-y}M_yO_{12}$ with $M=$Ge, Sn and $x,y<0.45$ has been investigated in the temperature range 4.2 K $\leq T \leq T_C$ at $\lambda=633$ nm and in the wavelength range 450 nm $\leq \lambda \leq$ 700 nm at $T=295$ K. The temperature variation of the ellipticity exhibits a characteristic minimum between 300 and 500 K and differs significantly from that of the Faraday rotation. The theory predicts a variation of the ellipticity being governed by the sublattice magnetizations which is in qualitative agreement with the experimental results. The sublattice magnetizations were deduced from the fit of the molecular-field theory to the measured saturation magnetization data. From the wavelength dependence of the ellipticity it can be concluded that exclusively the divalent lead ions cause the magneto-optical effects. Their contribution to the ellipticity $\Delta\psi_F/x_{Pb^{2+}}$ expressed in deg/cm was found to be -6×10^4 at $\lambda=514$ nm and $T=295$ K.

I. INTRODUCTION

The Faraday rotation and the Faraday ellipticity are the two fundamental properties which characterize the magneto-optical behavior of magnetic materials. The knowledge of their temperature and wavelength dependence, therefore, is of great interest for the interpretation of the basic phenomena and for the development of technical applications.[1–3] For magnetic oxides, and, in particular, for garnets only the two ions Bi^{3+} and Pb^{2+} which exhibit an isoelectronic configuration are known to induce a large Faraday rotation owing to their influence on the octahedral iron transitions via an increase of the superexchange interaction.[4–8] The available data of the Faraday rotation of Bi- and Pb-substituted iron garnets display very similar features and therefore suggest that the basic mechanisms causing the magneto-optical effects are the same for both ions.

Unfortunately very little information is available on the Faraday ellipticity being related to the magnetic circular dichroism. Some results have been reported concerning the wavelength dependence[5,7,9] but the temperature dependence has not yet been investigated except for pure yttrium iron garnet.[10] Since the ellipticity and the rotation are independent quantities it is necessary to know the dependence on temperature and wavelength for both in order to obtain a more complete picture of the magneto-optical effects induced by the lead. Therefore, we have investigated the Faraday ellipticity of a series of lead-substituted gadolinium iron garnet films with respect to these properties. In Sec. II the theoretical background is summarized and in Sec. III the experimental results are presented. In Sec. IV the experimental data are compared with the theory and the magneto-optical behavior is discussed in terms of the possible transitions involved and compared with those of the Bi^{3+} ions.

II. THEORY

The magneto-optical effects can be described by a complex rotation Φ of the elliptically polarized transmitted light beam with respect to the incident beam.[4,11] The Faraday rotation θ_F and the angle ψ_F corresponding to the ellipticity ϵ_F are related to the real and imaginary part of Φ, respectively, and can be expressed as

$$\theta_F=\mathrm{Re}(\Phi/L),\quad \psi_F=\mathrm{Im}(\Phi/L)\ ,\qquad \epsilon_F=\tanh\psi_F\ , \tag{1}$$

where θ_F and ψ_F are defined per unit length. The complex rotation is composed of a magnetic dipole (Φ_m) and an electric dipole (Φ_e) transition given by

$$\Phi_m=\frac{2\pi\bar{n}}{c}\sum_1\hat{\gamma}_1M_1\ , \tag{2a}$$

$$\Phi_e=-\frac{\omega}{2c}(N_+-N_-)\ . \tag{2b}$$

The sum extends over the magnetic sublattices $M_1(T)$. $\bar{n}$, $\hat{\gamma}_1$, c, and ω are the mean refractive index, the complex gyromagnetic ratio of sublattice 1, the velocity, and frequency of the light, respectively. N_+ and N_- denote the complex refractive indices for right- and left-handed circularly polarized light, respectively. Since the main contributions originate from the electric dipole transitions, θ_F and ψ_F essen-

tially are governed by the real and imaginary part of $N_+ - N_-$ being related to the components of the dielectric tensor

$$\vec{\vec{\epsilon}} = \begin{pmatrix} \epsilon_{11} & i\epsilon_{12} & 0 \\ -i\epsilon_{12} & \epsilon_{11} & 0 \\ 0 & 0 & \epsilon_{33} \end{pmatrix} ,$$

which for garnets with $\vec{M} \| z$ is gyrotropic.[4,12,13] $N_\pm$ can be expressed by

$$N_\pm^2 = \epsilon_{11} \pm \epsilon_{12} . \tag{3}$$

Using the definitions

$$\begin{aligned} N_\pm &= n_\pm - ik_\pm , \\ \epsilon_{jk} &= \epsilon'_{jk} + i\epsilon''_{jk} , \\ \bar{n} &= \tfrac{1}{2}(n_+ + n_-), \quad \bar{k} = \tfrac{1}{2}(k_+ + k_-) , \end{aligned} \tag{4}$$

where $\bar{k}$ denotes the mean extinction coefficient, the contribution from the electric dipole transitions to the Faraday rotation θ_F^e and the ellipticity $\epsilon_F^e = \tanh\psi_F^e$ can be written as follows[4,11]:

$$\begin{aligned} \theta_F^e &= -\frac{\omega}{2c(\bar{n}^2 + \bar{k}^2)} (\bar{n}\epsilon'_{12} - \bar{k}\epsilon''_{12}) , \\ \psi_F^e &= -\frac{\omega}{2c(\bar{n}^2 + \bar{k}^2)} (\bar{k}\epsilon'_{12} + \bar{n}\epsilon''_{12}) . \end{aligned} \tag{5}$$

From Eqs. (5) it is obvious that the magneto-optical effects solely are controlled by the real and imaginary part of ϵ_{12}. This dielectric tensor component is determined by the transitions occurring between the ground states $|g\rangle$ and the excited states $|e\rangle$ and is given by[12]

$$\epsilon_{12} = -\frac{2\pi e^2(\bar{n}^2+2)^2}{9m} \sum_1 N_1 \sum_{g,e} w_g(1)\,\Omega_{eg}(1)[f_{eg}^-(1) - f_{eg}^+(1)] , \tag{6}$$

where

$$\Omega_{eg}(1) = \frac{1}{\omega_{eg}(1)} \frac{\omega - i\Gamma_{eg}(1)}{\omega_{eg}^2(1) - \omega^2 + \Gamma_{eg}^2(1) + 2i\omega\Gamma_{eg}(1)} . \tag{7}$$

m denotes the electron mass and the factor $(\bar{n}^2+2)^2/9$ accounts for the Lorentz-Lorenz correction. g runs over the ground states with occupation probability $w_g(1)$ and e runs over excited states at energies $\hbar\omega_{eg}(1)$ having linewidth $\Gamma_{eg}(1)$ at sublattice 1. N_1 is the number of absorbing centers per unit volume and $f_{eg}^\pm(1)$ are the oscillator strengths

$$f_{eg}^\pm(1) = \frac{m\omega_{eg}(1)}{\hbar e^2} P_{eg}^\pm(1) \tag{8}$$

for transitions occurring via right- and left-handed circular polarizations. $P_{eg}^\pm(1)$ are the matrix elements of the electric dipole moment operators

$$P_{eg}^\pm(1) = e^2 |\langle e|x_1 \pm iy_1|g\rangle|^2 . \tag{9}$$

Combining Eqs. (6), (7), and (8) ϵ'_{12} and ϵ''_{12} can be calculated yielding

$$\epsilon'_{12} = -\frac{2\pi(\bar{n}+2)^2}{9\hbar\omega} \sum_1 N_1 \sum_{g,e} w_g(1) p'_{eg}(1)[P_{eg}^-(1) - P_{eg}^+(1)] , \tag{10a}$$

$$\epsilon''_{12} = \frac{2\pi(\bar{n}^2+2)^2}{9\hbar\omega} \sum_1 N_1 \sum_{g,e} w_g(1) p''_{eg}(1)[P_{eg}^-(1) - P_{eg}^+(1)] , \tag{10b}$$

where

$$\begin{aligned} p'_{eg}(1) &= \omega\omega_{eg}(1)\,\mathrm{Re}\,\Omega_{eg}(1) , \\ p''_{eg}(1) &= \omega\omega_{eg}(1)\,\mathrm{Im}\,\Omega_{eg}(1) . \end{aligned} \tag{11}$$

For the off-resonance low-frequency region the sums over the ground and excited states in Eqs. (10a) and (10b) can be related to the sublattice magnetization[14]:

$$\sum_{g,e} w_g(1) p'_{eg}(1)[P_{eg}^-(1) - P_{eg}^+(1)] = K_l p_l(\omega) M_l(T) . \tag{12}$$

A corresponding expression holds for the sum in Eq. (10b). $p_l'(\omega)$ and $p_l''(\omega)$ represent the frequency dependence and are related to $p'_{eg}(l)$ and $p''_{eg}(l)$, respectively. The K_l are constants.

Combining Eqs. (1), (2), (5), (9), (10), and (12), it turned out that both $\theta_F = \theta_F^m + \theta_F^e$ and $\psi_F^e = \psi_F^m + \psi_F^e$ are related in the same way to the magnetic sublattice magnetizations $M_a(T)$ (octahedral), $M_d(T)$ (tetrahedral), and $M_c(T)$ (dodecahedral) and are given by

$$\theta_F(T) = A(\omega)M_a(T) + D(\omega)M_d(T) + C(\omega)M_c(T) \ , \tag{13a}$$

$$\psi_F(T) = a(\omega)M_a(T) + d(\omega)M_d(T) + c(\omega)M_c(T) \ . \tag{13b}$$

The magneto-optical coefficients a, A; d, D; and c, C depend on frequency but are temperature independent provided the temperature dependence of $\bar{n}$, $\bar{k}$, and $\Gamma_{eg}(1)$ is negligible. The coefficients are related to the quantities introduced in Eqs. (1), (2), (5), (11), and (12) by

$$L(\omega) = \frac{2\pi\bar{n}}{c}\left[\gamma_1 + \eta_1 \frac{(\bar{n}^2+2)^2 N_1}{18\hbar\bar{n}^2(1+q^2)} K_l[p_l'(\omega) + qp_l''(\omega)]\right] \ , \tag{14a}$$

$$1(\omega) = \frac{2\pi\bar{n}}{c}\left[\lambda_1 + \eta_1 \frac{(\bar{n}^2+2)^2 N_1}{18\hbar\bar{n}^2(1+q^2)} K_l[qp_l'(\omega) - p_l''(\omega)]\right] \ , \tag{14b}$$

where $q = \bar{k}/\bar{n}$ and $\gamma_l = \mathrm{Re}\hat{\gamma}_1$. $\lambda_1 = \mathrm{Im}\hat{\gamma}_1$ is the damping constant and can be related to the ferromagnetic resonance linewidth. $L = A,D,C$ and $l = a,d,c$ refer to octahedral, tetrahedral, and dodecahedral sites, respectively. η_1 accounts for the sign of the sublattice moments where $\eta_d = 1$ and $\eta_a = \eta_c = -1$.

For the magneto-optical effects induced by Pb^{2+} and Bi^{3+} the transitions are of the diamagnetic type (orbitally nondegenerate ground state and orbitally degenerate excited states).[4,14] Assuming the level spacing of the ground and excited states to be small as compared to the separation $\hbar\omega_{0l}$ of the mean energies of ground and excited states the frequency dependence can be simplified considerably. In the energy region away from the transitions the frequency dependent terms of θ_F and ψ_F can be written as

$$p_l'(\omega) + qp_l''(\omega) = \frac{\hbar\omega_{0l}\Delta\omega(1)\omega^2}{(\omega_{0l}^2 - \omega^2)^2}\left[1 + q\frac{\Gamma(1)}{\omega} f(\omega,\omega_{0l})\right] \ , \tag{15a}$$

$$qp_l'(\omega) - p_l''(\omega) = \frac{\hbar\omega_{0l}\Delta\omega(1)\omega^2}{(\omega_{0l}^2 - \omega^2)^2}\left[q - \frac{\Gamma(1)}{\omega} f(\omega,\omega_{0l})\right] \ , \tag{15b}$$

where $f(\omega,\omega_{0l}) \sim 1 + r\omega_{0l}^2\omega^2(\omega_{0l}^2 - \omega^2)^{-2}$ and r is a constant. Since for the garnets investigated q and $\Gamma(1)/\omega$ are small compared to unity the frequency dependence of θ_F is simply given by $\theta_F \sim \omega^2(\omega_{0l}^2 - \omega^2)^{-2}$ while that of ψ_F is expected to be more complex.

TABLE I. Chemical analysis data of the investigated garnet films. The divalent-lead concentration is obtained from the condition of charge compensation.

Composition	Sample	x	y	z	$x_{Pb^{2+}}$
$Y_{3-x}Pb_xFe_{5-z}Pt_zO_{12}$	1	0.004	0	0.005	0.004
	2	0.010	0	0.010	0.010
$Gd_{3-x}Pb_xFe_{5-z}Pt_zO_{12}$					
	3	0.357	0	0.048	0.203
	4	0.125	0.124	0.014	0.125
$Gd_{3-x}Pb_xFe_{5-y-z}Sn_yPt_zO_{12}$	5	0.191	0.205	0.015	0.191
	6	0.325	0.243	0.024	0.296
	7	0.132	0.125	0.020	0.132
	8	0.263	0.171	0.029	0.232
$Gd_{3-x}Pb_xFe_{5-y-z}Ge_yPt_zO_{12}$					
	9	0.443	0.201	0.043	0.344
Error	. . .	±0.003 to ±0.009	±0.005 to ±0.010	±0.002 to ±0.005	±0.003 to ±0.010

III. EXPERIMENT

A. Garnet films

The garnet films of composition $Gd_{3-x}Pb_xFe_{5-y-z}M_yPt_zO_{12}$ with $M=Ge^{4+}$, Sn^{4+} were grown by liquid phase epitaxy from a bismuth-free $PbO\text{-}B_2O_3$ based flux[15] onto (111) oriented magnesium-, calcium-, and zirconium-substituted gadolinium gallium garnet substrates.[16] The growth temperature ranged between 1000 and 1200 K and the thickness of the films between 1.7 and 9.1 μm. The chemical analysis data for selected film compositions used for the temperature-dependent measurements are compiled in Table I. The platinum enters the lattice as an impurity and is assumed to occupy octahedral sites as a four-valent ion. The content of other impurities was below 0.005 per formula unit. The valence states of the lead and the corresponding concentrations are obtained from the condition of charge compensation yielding $x_{Pb^{2+}}=\frac{1}{2}(x+y+z)$ and $x_{Pb^{4+}}=\frac{1}{2}(x-y-z)$. Further information about the possible distribution of the Pb^{4+} ions over octahedral and dodecahedral sites can be extracted from a comparison of the calculated and measured compensation temperature and lattice mismatch.[7,8] The Ge^{4+} and Sn^{4+} ions are assumed to occupy exclusively tetrahedral and octahedral sites, respectively.

B. Magnetization

The comparison of the measured temperature dependence of the ellipticity with the theory according to Eq. (13b) requires the knowledge of the sublattice magnetizations. These can be obtained from the fit of the molecular-field theory to the measured saturation magnetization data based on the analysis data, the present valence states and the distribution of the ions over the different lattice sites.[7,17] For some films the magnetization already has been reported.[7] Therefore, the measured temperature dependence of $4\pi M_s$ is displayed in Fig. 1 only for a few samples to demonstrate the good fit which can be achieved.

The saturation magnetization was measured with a vibrating sample magnetometer in fields up to 1.6×10^6 A/m. The magnetization data were obtained by extrapolation to zero field and are compiled in Table II for $T=4.2$ and 295 K.

C. Faraday rotation

The temperature dependence of the Faraday rotation is displayed in Fig. 2 for $\lambda=633$ nm being already discussed in Refs. 7 and 8 except for sample 5. The solid lines represent the theory according to Eq. (13a) based on the sublattice magnetization inferred from the fit of the molecular-field theory to the mea-

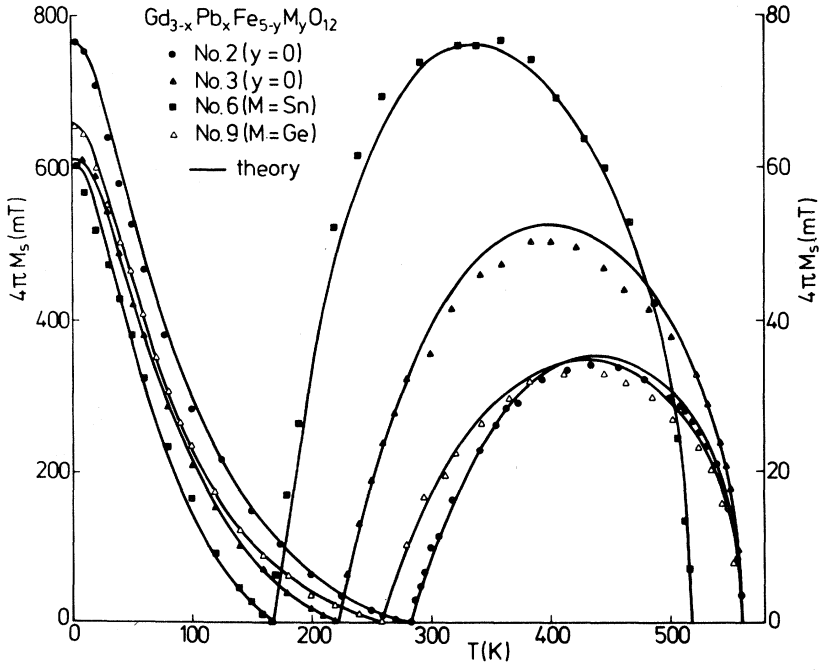

FIG. 1. Temperature dependence of the saturation magnetization. The data for $T < T_{comp}$ refer to the left scale and those for $T > T_{comp}$ to the right scale. The solid lines were calculated by means of the molecular-field theory.

TABLE II. Measured magnetic and magneto-optical (at $\lambda = 633$ nm) data for the garnet films investigated.

Sample	T_{comp} (K)	$T = 4.2$ K $4\pi M_s$ (mT)	θ_F (deg cm^{-1})	ψ_F (deg cm^{-1})	$T = 295$ K $4\pi M_s$ (mT)	θ_F (deg cm^{-1})	ψ_F (deg cm^{-1})
1	· · ·	247	275	−380	180	785	−540
2	283	771	200	0	7	345	−335
3	223	613	−2690	−2950	35	−2310	−2600
4	220	673	−1880	−130	35	−1450	−410
5	189	693	−3120	−280	40	−2410	−610
6	167	602	−4050	−1140	74	−3350	−1200
7	287	750	−1680	−244	4	−1430	−580
8	279	716	−2890	−1500	70	−2680	−1550
9	261	663	−4210	−1680	15	−3810	−2500

sured saturation magnetization. The very good description of the whole temperature variation for all samples was achieved with temperature independent magneto-optical coefficients A, D, and C defined in Eq. (13a) except for samples 2 and 3 where C was taken to depend on T.[7] The influence of Pb^{2+} on the octahedral iron transitions leads to a strong linear decrease of the octahedral magneto-optical coefficient corresponding to the effect of Bi^{3+}.[7] Thus θ_F decreases to negative values with increasing Pb^{2+} content. The concentration dependence of θ_F at $T = 295$ K for $\lambda = 633$ nm is shown in Fig. 3 for both ions. The contribution of the Bi^{3+} turned out to be roughly twice that of the Pb^{2+}.

The values for the rotation at $T = 4.2$ and 295 K are summarized in Table II.

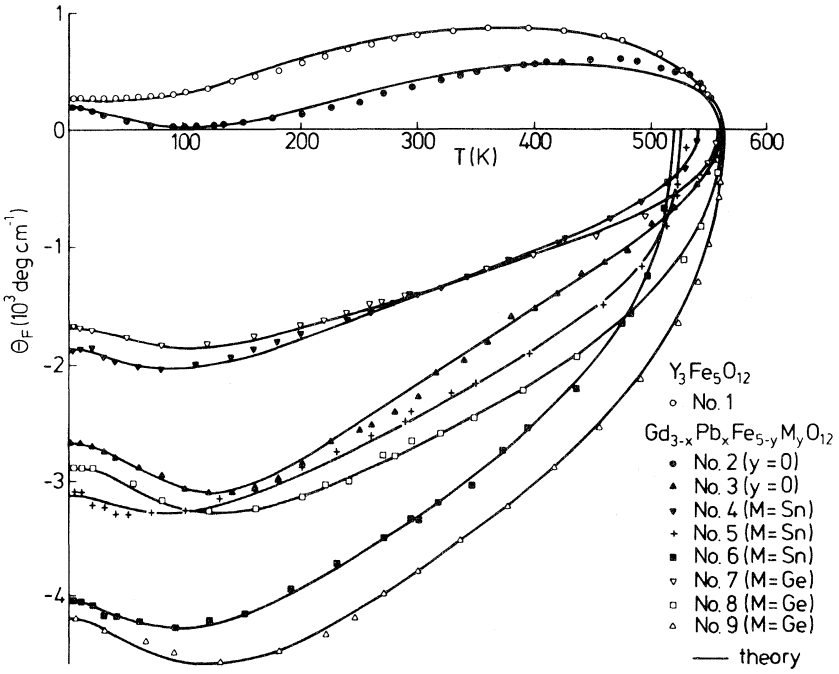

FIG. 2. Temperature dependence of the Faraday rotation at $\lambda = 633$ nm. The solid lines represent the theory according to Eq. (13a).

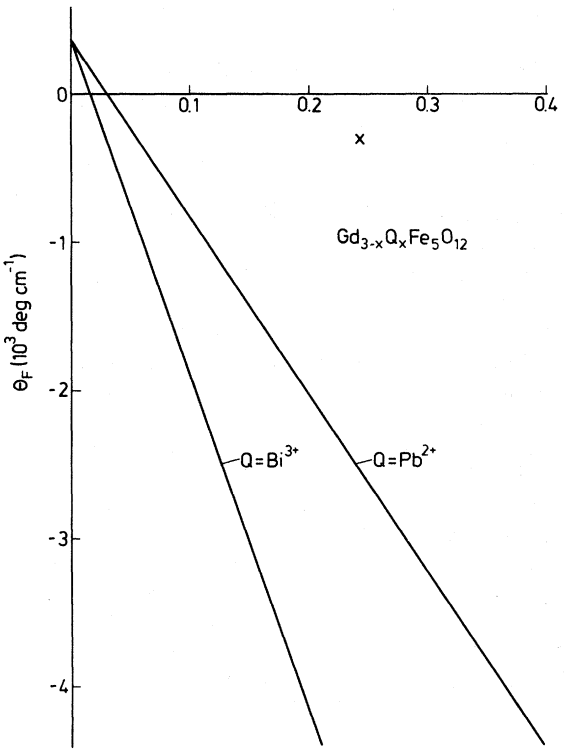

FIG. 3. Concentration dependence of the Faraday rotation for lead- and bismuth-substituted gadolinium iron garnets at $\lambda = 633$ nm and $T = 295$ K.

D. Faraday ellipticity

1. Experimental conditions

The wavelength dependence of the Faraday ellipticity ψ_F at room temperature was determined from the measured circular dichroism $\Delta\alpha = \alpha_+ - \alpha_- = (4\pi/180)\psi_F$ where α_+ and α_- denote the optical absorption coefficients for right- and left-handed circularly polarized light. α_+ and α_- were obtained from the hysteresis loop of the transmitted intensity using a Glan-Thomson polarizer and a well adjusted Babinet-Soleil compensator. In the short-wavelength range the monochromatic lines of an Ar^+ laser were used instead of the monochromator equipment with 6-nm resolution to account for the strong dispersion peak at $\lambda = 490$ nm.

The temperature dependence of ψ_F at $\lambda = 633$ nm was measured by means of an optical cryostat ($4.2 \leq T \leq 300$ K) and an oven ($300\ \text{K} \leq T \leq T_C$). The polarimeter equipment was supplied with an automatic nulling procedure.[18] A quarter-wave plate behind the sample being adjusted with its axis parallel to the incident polarization transforms ψ_F directly into a rotation of the azimuth measured by a rotation of the analyzer until minimum transmitted intensity is reached. Some problems arose from the stress-induced birefringence of the four windows of the cryostat and the two of the oven. Although the windows had been carefully selected and mounted a maximum variation of the ψ_F values of up to 1° could occur when the azimuth of the incident polarization was rotated by 360°. Therefore, the azimuth of the incident polarization was chosen such that ψ_F data at room temperature measured with and without cryostat or oven are in agreement within 10%. An additional source for errors is the birefringence of the substrates.

The hysteresis loops of the ellipticity were measured in fields up to 1.3×10^6 A/m and the reported ψ_F values were derived from extrapolation to zero field.

2. Experimental results

The wavelength dependence of the ellipticity is shown in Fig. 4 for some of the lead-substituted films and for one bismuth-substituted film (dashed line). The lead films are characterized by a strong peak around 490 nm while in the case of the bismuth this peak occurs around 450 nm.[5,7] For longer wavelength the Pb^{2+} ions obviously give rise to a higher contribution to ψ_F than the Bi^{3+} ions. Further a dif-

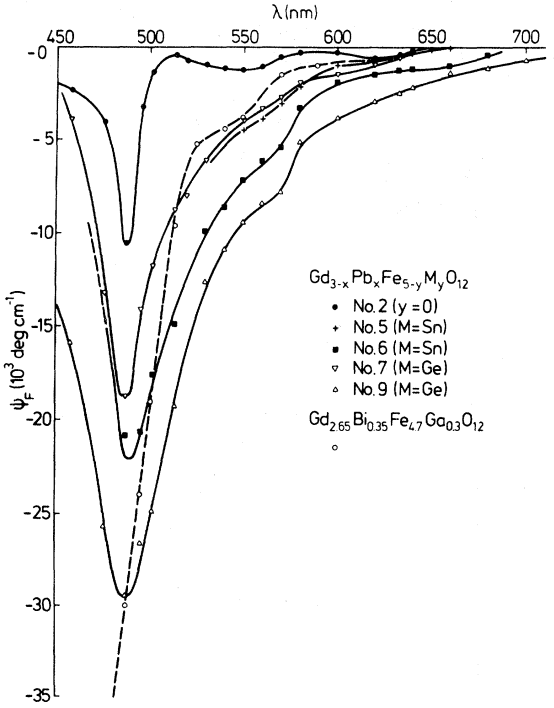

FIG. 4. Wavelength dependence of a bismuth-substituted gadolinium iron garnet film (dashed line) and of lead-substituted gadolinium iron garnet films (solid lines) at $T = 295$ K.

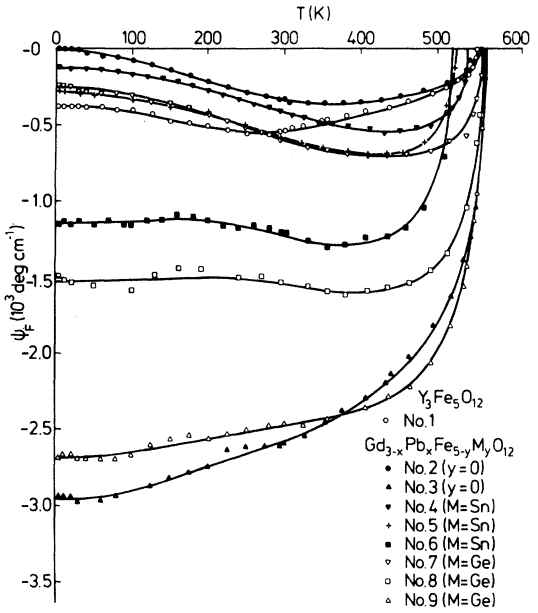

FIG. 5. Temperature dependence of the Faraday ellipticity for a yttrium iron garnet film and lead-substituted gadolinium iron garnet films at $\lambda = 633$ nm.

ferent behavior is present for different charge compensations of the Pb^{2+} ions. For those garnets where $x_{Pb^{4+}} = 0$ a lower value for $|\psi_F|$ is found than for compositions with $x_{Pb^{4+}} > 0$ which becomes evident from a comparison of samples 4 and 7. For compositions with higher Pb^{4+} content ψ_F even can become

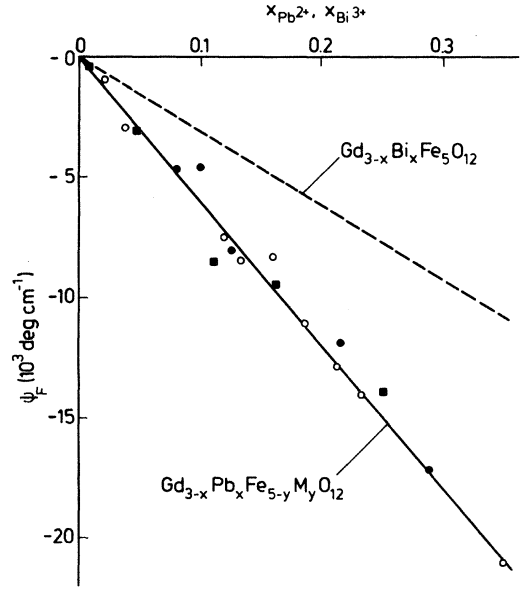

FIG. 6. Concentration dependence of the Faraday ellipticity for lead- and bismuth-substitued gadolinium iron garnets at $\lambda = 514$ nm and $T = 295$ K. The symbols ○, ●, and ■ refer to compositions where charge compensation is maintained by $Ge^{4+}+Pb^{4+}$, $Sn^{4+}+Pb^{4+}$, and Pb^{4+}, respectively.

comparable in magnitude with θ_F for longer wavelengths.

The temperature dependence of ψ_F has been measured at $\lambda = 633$ nm and is presented in Fig. 5. All samples with a low lead content exhibit a minimum occurring between $T = 350$ and 500 K except for yttrium iron garnet where the minimum was found around $T \approx 250$ K. While for $Y_3Fe_5O_{12}$ the temperature dependence of ψ_F and θ_F is similar it differs considerably for lead-substituted garnets. In particular, the shift of the minimum of ψ_F to higher temperatures and the steep decrease at the Curie temperature in comparison to the M_s and θ_F variations are typical features of ψ_F which have to be attributed to the lead.

The concentration dependence of ψ_F is displayed in Fig. 6 at $T = 295$ K and $\lambda = 514$ nm since at this wavelength ψ_F is of comparable magnitude for lead and bismuth which for the latter at $\lambda = 633$ nm becomes very small (see Fig. 4). The linear relationship again confirms that the magneto-optical behavior of lead-substituted garnets has to be attributed exclusively to the Pb^{2+} ions. The optical absorption α also increases linearly with increasing Pb^{2+} content yielding $\Delta\alpha/x_{Pb^{2+}} = 4.2 \times 10^4$ cm^{-1} at $\lambda = 514$ nm.

IV. DISCUSSION

A. Wavelengths dependence

Pb^{2+} and Bi^{3+} ions cause large Faraday rotations owing to their influence on the octahedral iron transitions via a significantly increased superexchange interaction. The wavelength and temperature dependence of θ_F show comparable characteristics for both ions. From the frequency dependence expressed by Eq. (15a) for one sublattice a wavelength dependence of the contribution of the Pb^{2+} ions to the rotation $\Delta\theta_F = \theta_F(x_{Pb^{2+}}) - \theta_F(x_{Pb^{2+}} = 0)$ according to the relation

$$\Delta\theta_F(\lambda) = \vartheta_F(T)\frac{\lambda_0^2\lambda^2}{(\lambda^2 - \lambda_0^2)^2} \tag{16}$$

is expected where $\vartheta_F(T)$ represents the frequency-independent quantities. Therefore a plot of $\lambda\Delta\theta_F^{-1/2}$ versus λ^2 should give information about the position of the transitions being responsible for the magneto-optical effects. For samples 6, 8, and 9 a linear relation results as shown in Fig. 7. From the extrapolation to zero for $\lambda\Delta\theta^{-1/2}$ λ_0 was deduced to be approximately 412 nm which is in good agreement with the result for bismuth iron garnets where λ_0 was found to be 417 nm.[19] The frequency dependence of ψ_F is more complicated. Away from the absorption center Eq. (15b) predicts ψ_F to vary as

$$\omega^2(\omega_0^2 - \omega^2)^{-2}[q - \Gamma f(\omega_0, \omega)/\omega]$$

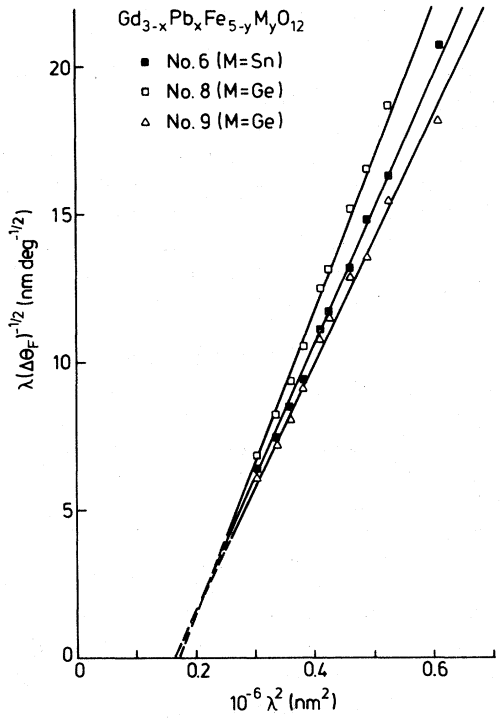

FIG. 7. Wavelength dependence of the modified Faraday rotation for lead-substituted gadolinium iron garnet films (see text).

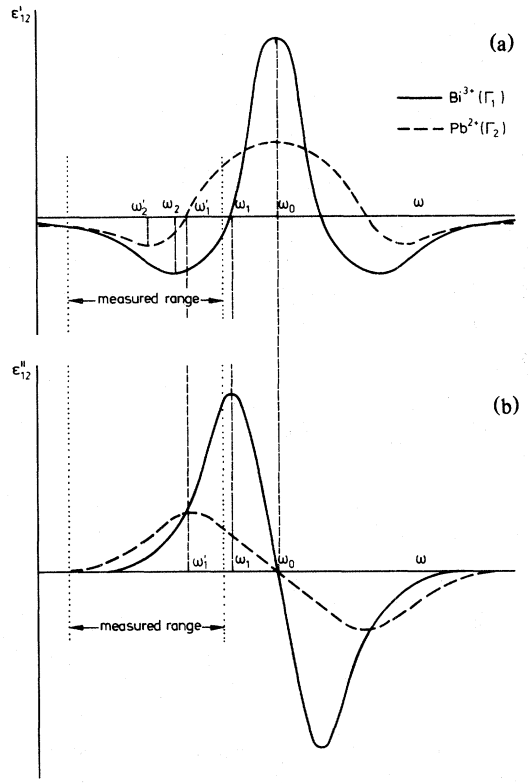

FIG. 8. Schematic representation of the frequency dependence of (a) the real (ϵ'_{12}) and (b) the imaginary part (ϵ''_{12}) of the off-diagonal dielectric tensor component for the case of a diamagnetic transition. The solid and dashed curves account for a lower (Γ_1) and higher (Γ_2) value of the linewidth, respectively (see text).

assuming $\Gamma(1)=\Gamma$. Since

$$f(\omega_0,\omega)\sim 1+r\omega_0^2\omega^2(\omega_0^2-\omega^2)^{-2}$$

there are three different frequency terms. If one of these dominates a wavelength dependence similar to Eq. (16) is expected. A comparison with the experimental data, however, shows a more complicated behavior suggesting a mixing of the different terms.

From the results reported in our previous work[7,8] and from the measured wavelength dependence of the ellipticity it can be concluded that the magneto-optical behavior originating from the Pb^{2+} ions can be interpreted in analogy with that of the Bi^{3+} ions in garnets. The principal frequency dependence of ϵ'_{12} and ϵ''_{12} according to Eqs. (10) is sketched in Fig. 8 for a diamagnetic transition at ω_0 which applies for the optical transitions of the trivalent iron ions. Here it should be noticed that the signs of θ_F and ψ_F are related to ϵ'_{12} and ϵ''_{12} via Eqs. (5) as shown in Fig. 8 provided only one sublattice contribution dominates. This applies for $Y_3Fe_5O_{12}$ and $Gd_3Fe_5O_{12}$ where the octahedral sublattice gives the main contribution. Otherwise the signs of θ_F, ψ_F and ϵ'_{12}, ϵ''_{12} are correlated in a more complex manner owing to the different sublattice contributions. The solid and dashed lines in Fig. 8 correspond to different values of the linewidth Γ. For the higher Γ_2 (dashed line) the following significant differences in the frequency dependence occur with respect to the Γ_1 case: (i) reduction of $\theta_F\sim-\epsilon'_{12}$ around the extrema at ω_0 and ω_2, a shift of $\omega_1(\theta_F=0)$ and ω_2 towards lower frequencies, (ii) reduction of $\psi_F\sim-q\epsilon'_{12}-\epsilon''_{12}$ around ω_0 and a rise of ψ_F for $\omega>>\omega_0$, a shift of ω_1 (extremum of ψ_F) towards lower frequencies. These changes of the spectra of θ_F and ψ_F for the Pb^{2+}-substituted garnets as compared to those of the Bi^{3+}-substituted garnets indeed are observed. For Pb^{2+} θ_F at ω'_2 is reduced by a factor of 5 (Ref. 7) and ψ_F at ω'_1 approximately by a factor of 2.5 (Fig. 4, Ref. 5) compared to the corresponding values of Bi^{3+} at ω_2 and ω_1. For $\omega<\omega'_1$ the Pb^{2+} contribution to ψ_F is larger than that for Bi^{3+} (Fig. 6) and the wavelength shift corresponding to $\omega_1-\omega'_1$ was found to be approximately 40 nm (Fig. 7, Ref. 19). This agreement between theory and experiment indicates that the two ions Pb^{2+} and Bi^{3+} enhance the same iron transitions which leads to similar magneto-optical effects. The differences in the wavelength dependence can be attributed to a larger linewidth of the iron transitions in the lead case.

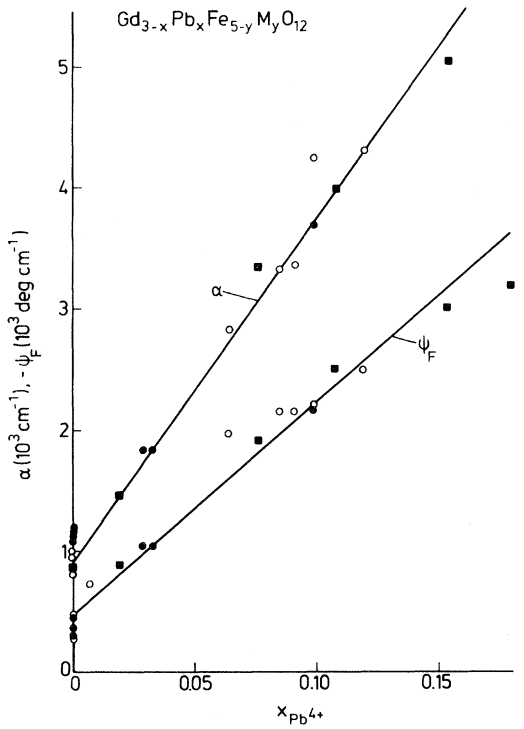

FIG. 9. Variation of the optical absorption and the Faraday ellipticity with the Pb^{4+} content at $\lambda = 633$ nm and $T = 295$ K. The symbols ○, ●, and ■ refer to compositions where charge compensation is maintained by $Ge^{4+}+Pb^{4+}$, $Sn^{4+}+Pb^{4+}$, and Pb^{4+}, respectively.

Although the origin of the magneto-optical effects in these materials has to be attributed solely to the divalent lead ions small differences in the wavelength dependence are present with respect to the different charge compensating ions.[8] The differences for compositions with Pb^{2+}, Ge^{4+} and Pb^{2+}, Sn^{4+} where $x \approx y+z$ are of minor importance but for those compositions where $x \neq y+z$ and a self-compensation occurs for a significant part of the lead considerably higher values of θ_F and ψ_F are observed for $\lambda \gtrsim 600$ nm. In this wavelength range a direct relation to the Pb^{4+} content was found as shown in Fig. 9 for the optical absorption and the Faraday ellipticity at $\lambda = 633$ nm and $T = 295$ K. This suggests that a charge transfer mechanism between the lead ions or the iron ions is involved which also may cause the higher linewidth.

For garnets containing Pb^{2+} and Pb^{4+} the higher θ_F and ψ_F values as compared to Bi^{3+} might be of some interest for technical applications in the infrared.

B. Temperature dependence

The temperature dependence of ψ_F is expected to be governed by the sublattice magnetizations according to Eq. (13b). These sublattice magnetizations being expressed in Bohr magnetons per two formula units were obtained from the fit of the molecular-field theory to the measured saturation magnetization (Fig. 1) as discussed in Sec. III B. The comparison of the theory and the experimental ψ_F data of Fig. 5 are shown in Fig. 10 assuming the coefficients a, d, and c to be temperature independent. For c the same value has been used for all compositions except for $Y_3Fe_5O_{12}$ where $c = 0$. These coefficients are listed in Table III for some samples. A satisfactory fit of the experimental data was achieved for the samples with a low lead content while the deviation between experiment and theory is significant for those with a high lead content which is in contrast to the case of the Faraday rotation (Fig. 2). In particular, the occurrence of the shallow minimum of ψ_F at relatively high temperatures which is not present for $\theta_F(T)$ indicates a temperature dependence of the coefficients a and d. Inspection of Eq. (14b) shows that different sources for a variation of the coefficients with T can be considered. The magnetic part via λ_1 is related to the resonance linewidth and therefore is a function of T. This contribution, however, is negligible with respect to the second term in Eq. (14b) originating from the electric dipole transitions. The mean refractive index $\bar{n}$, the mean extinction coefficient $\bar{k}$, and linewidth $\Gamma(1)$, however, are also functions of temperature and may be responsible for these differences between theory and experiment. In particular, $\bar{k}$ and $\Gamma(1)$ are expected to increase with increasing T and thus would tend to shift the calculated maximum towards higher temperatures which would improve the

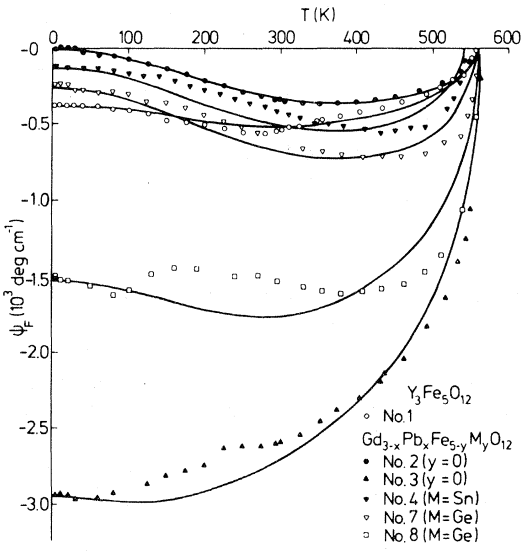

FIG. 10. Temperature dependence of the ellipticity at $\lambda = 633$ nm. The solid lines represent the theory according to Eq. (13b) assuming the coefficients a, d, and c to be temperature independent.

TABLE III. Magneto-optical coefficients of the Faraday ellipticity expressed in μ_B^{-1} deg cm^{-1}.

Sample	a	d	c
1	−141.2	81.5	. . .
2	−232.3	150.4	
3	−125.4	−19.8	
4	−249.7	146.2	2.74
8	−454.6	260.1	

agreement with the measured data. Since no experimental results about the temperature behavior of these quantities are available this problem could not be solved. Therefore, the values of the coefficients given in Table III can be regarded as a rough estimate only. They demonstrate, however, that in accordance with those being related to the Faraday rotation[7,8] the octahedral coefficient is much more affected by the lead ions than the tetrahedral coefficient. To extract the Pb^{2+} dependence of these coefficients a correction with respect to the tetrahedral and octahedral substitutions is necessary but this requires a higher accuracy of the values of a, d, and c.

V. CONCLUSIONS

The wavelength and temperature dependence of the Faraday ellipticity of lead-substituted gadolinium iron garnets can be interpreted in terms of enhanced iron transitions in correspondence to respective bismuth garnets. Thereby, the main differences of the observed magneto-optical effects induced by the divalent lead can be explained on the basis of a larger linewidth of the optical transitions involved as compared to that for the bismuth case. Small differences of the wavelength dependence originate from different charge compensation of the Pb^{2+} ions. In particular, compositions exhibiting self-compensation of the lead are expected to be characterized by higher values of the rotation and ellipticity in the infrared.

The temperature dependence of the ellipticity measured at $\lambda = 633$ nm is very different from that of the rotation and shows a minimum at relatively high temperatures. For low lead concentrations good agreement was found with the theory predicting a variation in terms of the sublattice magnetizations. For higher lead concentrations the deviation between theory and experiment becomes more significant which can be attributed to a temperature dependence of the magneto-optical coefficients. Further, these coefficients are affected by the Pb^{2+} ions such that the octahedral coefficient is much stronger reduced than the tetrahedral coefficient and therefore essentially causes the pronounced increase of the Faraday ellipticity which is in accordance with the situation for the Faraday rotation.

ACKNOWLEDGMENTS

The authors would like to thank G. Bartels, I. Bartels, and W. Tolksdorf for the growth and preparation of the garnet films, P. Willich for the chemical analysis, and J. Schuldt for technical assistance. Helpful discussions with H. Heitmann, J.-P. Krumme, and M. Urner-Wille are gratefully acknowledged.

[1]B. Hill and K.-P. Schmidt, Philips J. Res. 33, 211 (1978).
[2]B. Hill and K.-P. Schmidt, SID J. 10, 80 (1979).
[3]J. J. Krebs, W. G. Maisch, G. A. Prinz, and D. W. Forester, IEEE Trans. Magn. 16, 1179 (1980).
[4]G. B. Scott and D. E. Lacklison, IEEE Trans. Magn. 12, 292 (1976).
[5]S. Wittekoek, T. J. A. Popma, J. M. Robertson, and P. F. Bongers, Phys. Rev. B 12, 2777 (1975).
[6]H. Takeuchi, Jpn. J. Appl. Phys. 14, 1903 (1975).
[7]P. Hansen, H. Heitmann, and K. Witter, Phys. Rev. B 23, 6085 (1981).
[8]P. Hansen, W. Tolksdorf, and K. Witter, IEEE Trans. Magn. 17, 3211 (1981).
[9]G. B. Scott, D. E. Lacklison, H. I. Ralph, and J. L. Page, Phys. Rev. B 12, 2562 (1975).
[10]H. Toda and Y. Kakagawa, Jpn. J. Appl. Phys. 18, 2081 (1981).
[11]J. Dillon, in *Physics of Magnetic Garnets,* edited by A. Paoletti (North-Holland, New York, 1978), p. 379.
[12]F. J. Kahn, P. S. Pershan, and J. P. Remeika, Phys. Rev. 186, 891 (1969).
[13]J. F. Dillon, J. P. Remeika, and C. R. Staton, J. Appl. Phys. 41, 4613 (1970).
[14]W. A. Crossley, R. W. Cooper, J. L. Page, and R. P. van Stapele, Phys. Rev. 181, 896 (1969).
[15]W. Tolksdorf *et al.* (private communication); the relationship between the growth conditions and the composition of these films are planned to be discussed in another paper.
[16]D. Mateika, R. Laurien, and Ch. Rusche, J. Cryst. Growth (in press).
[17]P. Röschmann and P. Hansen, J. Appl. Phys. 52, 6257 (1981).
[18]R. M. A. Azzam and N. M. Bashara, *Ellipsometry and Polarized Light* (North-Holland, Amsterdam-New York-Oxford, 1977).
[19]G. B. Scott, D. E. Lacklison, and J. L. Page, J. Phys. C 8, 519 (1975).